Equilibrium and Kinetic Studies of the Interactions of a Porphyrin with Low-Density Lipoproteins

Stéphanie Bonneau,*† Christine Vever-Bizet,*† Patrice Morlière,*‡ Jean-Claude Mazière,§ and Daniel Brault*†
*Laboratoire de Photobiologie and †CNRS UMR 8646, Muséum National d'Histoire Naturelle, 75231 Paris Cedex 05, France; ‡INSERM U532, Institut de Recherche sur la Peau, Hôpital Saint Louis, 75475 Paris Cedex 10, France, and §Service de Biochimie, Hôpital Nord d'Amiens, 80054 Amiens Cedex 01, France

ABSTRACT Low-density lipoproteins (LDL) play a key role in the delivery of photosensitizers to tumor cells in photodynamic therapy. The interaction of deuteroporphyrin, an amphiphilic porphyrin, with LDL is examined at equilibrium and the kinetics of association/dissociation are determined by stopped-flow. Changes in apoprotein and porphyrin fluorescence suggest two classes of bound porphyrins. The first class, characterized by tryptophan fluorescence quenching, involves four well-defined sites. The affinity constant per site is 8.75×10^7 M^{-1} (cumulative affinity 3.5×10^8 M^{-1}). The second class corresponds to the incorporation of up to 50 molecules into the outer lipidic layer of LDL with an affinity constant of 2×10^8 M^{-1}. Stopped-flow experiments involving direct LDL porphyrin mixing or porphyrin transfer from preloaded LDL to albumin provide kinetic characterization of the two classes. The rate constants for dissociation of the first and second classes are 5.8 and 15 s^{-1}; the association rate constants are 5×10^8 M^{-1} s^{-1} per site and 3×10^9 M^{-1} s^{-1}, respectively. Both fluorescence and kinetic analysis indicate that the first class involves regions at the boundary between lipids and the apoprotein. The kinetics of porphyrin-LDL interactions indicates that changes in the distribution of photosensitizers among various carriers could be very sensitive to the specific tumor microenvironment.

INTRODUCTION

The retention of certain porphyrins by solid tumors, as compared to normal surrounding tissues, has been recognized for many years. This retention and the ability of these molecules to generate short-lived toxic species upon light irradiation are at the basis of a selective therapeutic approach, photodynamic therapy (PDT). In recent years, this therapy has benefited from the development of lasers and optical fibers and is now an established procedure for the treatment of certain cancers (Pass, 1993; Dougherty et al., 1998). Regulatory approval for PDT with a porphyrin-based preparation, Photofrin, has been given. Second-generation photosensitizers are now being developed with improved light absorption in the red region (Boyle and Dolphin, 1996). Although various factors come into play in the overall efficiency of PDT, correlation has been established between the lipophilic character of photosensitizers and their accumulation in tumors (Henderson et al., 1997) and, consequently, their photosensitizing efficiency (Lavi et al., 2002).

It has been well established that the affinity of lipophilic photosensitizers for serum lipoproteins, in particular low-density lipoproteins (LDL), plays an important role in the delivery of these drugs to tumor cells (Jori et al., 1984; Reyftmann et al., 1984; Candide et al., 1986; Kessel, 1986). The physiological role of LDL is providing cells with cholesterol via cellular uptake. This is achieved by receptor-mediated endocytosis resulting in the delivery of components of LDL to the lysosomal compartment (Brown and Goldstein, 1976). The distribution pattern of some porphyrins has been found to be correlated with the relative numbers of LDL receptors in different tissues (Kessel, 1986). Several authors have pointed out an increased cholesterol catabolism and over-expression of LDL receptors in tumor cells (Gal et al., 1981; Vitols et al., 1992). The cellular uptake and photoactivity of porphyrins have been increased through potentialization of LDL catabolism by lovastatin (Biade et al., 1993). By contrast, PDT-resistant tumor cells exhibit low activity of LDL-related receptors (Luna et al., 1995). These data taken together suggest that the selectivity of lipophilic photosensitizing antitumoral agents arises from a favored low-density lipoprotein receptor pathway (Maziere et al., 1991). This specific pathway also plays a key role in the mechanism of other PDT modalities used to treat atherosclerotic lesions (de Vries et al., 1999) or to treat choroidal neovascularization associated with age-related macular degeneration (Miller et al., 1995).

Low-density lipoproteins are constituted of phospholipids, cholesterol (esterified or not), triglycerides, and the B100 apoprotein which contains, among other residues, 37 tryptophans and 151 tyrosines (Yang et al., 1986). A consensus model has been proposed (Segrest et al., 2001) consisting of a monolayer of phospholipids and cholesterol surrounding a lipid core made of triglycerides and cholesterol esters. Although the exact shape of LDL particles is still debated, they can be viewed as spherical with a diameter of 22 nm (Schumaker et al., 1994; Segrest et al., 2001). A tentative representation is shown in Fig. 1.

Drugs bound to LDL could be distributed among the three major components of these particles, i.e., the apoli-

Submitted April 4, 2002, and accepted for publication July 29, 2002.

Address reprint requests to Daniel Brault, Laboratoire de Photobiologie, CNRS UMR 8646, Muséum National d'Histoire Naturelle, 43 rue Cuvier, 75231 Paris Cedex 05, France. Tel.: 33-1-40793697; Fax: 33-1-40793705; E-mail: brault@mnhn.fr.

0006-3495/02/12/3470/12 $2.00

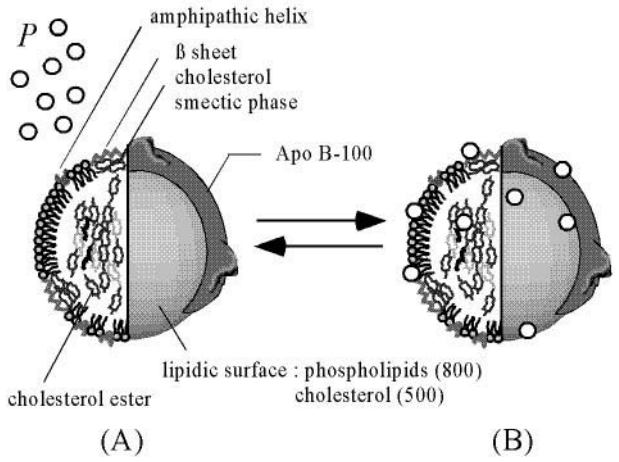

FIGURE 1 (*A*) Postulated structure of LDL; (*B*) potential sites of porphyrin binding.

poprotein, the phospholipid envelope, and the lipid core. The efficiency of LDL particles as carriers depends on the overall number of exogenous molecules they can bind. However, the integrity of the particle and, more particularly, that of the receptor-binding site on apoB100 must be preserved. It is of particular importance to consider the interactions from a dynamic point of view. The rates of exchange of the photosensitizer between LDL and the other serum proteins in blood must be considered. Indeed, the photosensitizer distribution may be modified by the particular environment provided by the interstitial compartment of neoplastic tissues (Jain, 1987), or even be modified in the course of the LDL endocytosis process.

The capacity of LDL to bind some photosensitizers and their functionality have been examined in a few studies (Reyftmann et al., 1984; Candide et al., 1986; Beltramini et al., 1987; de Smidt et al., 1993). Except for results on isolated rabbit lipoprotein fractions (Beltramini et al., 1987), no data are available concerning the distribution of porphyrins in the various LDL compartments. To our knowledge, no information about the dynamics of porphyrin interactions with LDL has been published so far.

In the present paper, we investigate the interaction of an amphiphilic porphyrin, deuteroporphyrin (DP), with LDL. This dicarboxylic porphyrin was chosen because its structure corresponds to the framework of the components of Photofrin, and approaches that of protoporphyrin, another photosensitizer of therapeutic interest. Moreover, it can be purified to a high degree and is less sensitive to photodegradation than protoporphyrin. The different classes of binding sites are identified and characterized by monitoring the intrinsic fluorescence of LDL or that of the porphyrin. The dynamics of the interactions of LDL and porphyrin and transfer to albumin are investigated using a stopped-flow apparatus. All these processes are shown to be fast. This approach has implications beyond the immediate problem

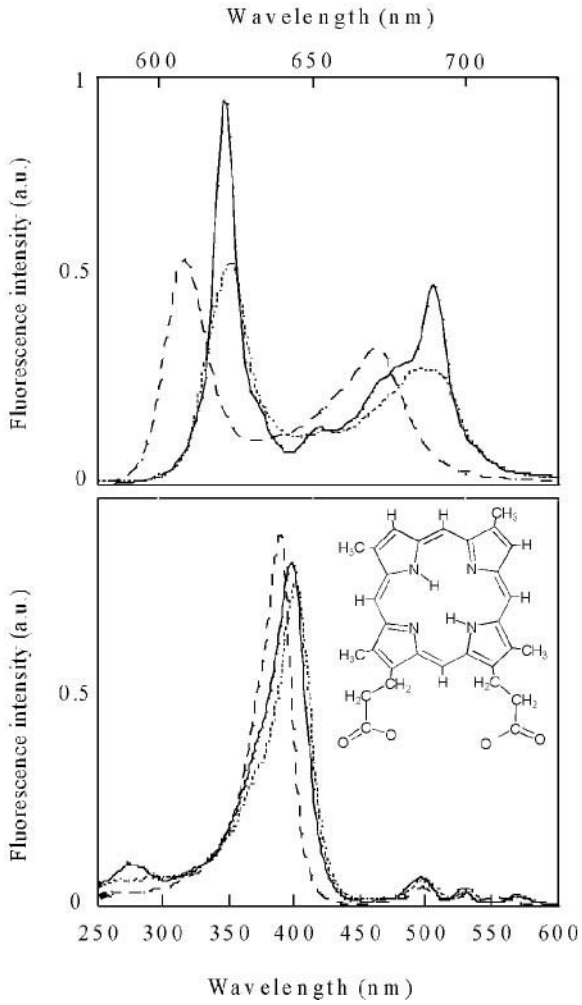

FIGURE 2 Structure of deuteroporphyrin (*inset*). Fluorescence emission (*top*) and excitation spectra (*bottom*) of 5×10^{-8} M deuteroporphyrin in phosphate buffer (*dashed line*), bound to 10^{-7} M LDL (*solid line*), and to excess (5×10^{-6} M) HSA (*dotted line*). Excitation and emission wavelengths were set at 396 and 625 nm for emission and excitation spectra, respectively.

of photosensitizer transport by endogenous lipoproteins, but also relates to the behavior of other drugs (Rudling et al., 1983; Shaw et al., 1987) as well as the design of artificial lipid particles for drug targeting (Rensen et al., 2001).

MATERIALS AND METHODS

Chemicals

All the experiments were carried out at pH 7.4 in saline phosphate buffer (PBS) prepared from Na_2HPO_4/KH_2PO_4 (total phosphate, 9.57×10^{-3} M), NaCl, 0.15 M and KCl, 2.68×10^{-3} M. Deuteroporphyrin (DP), the structure of which is shown in Fig. 2, was prepared as described previously (Brault et al., 1986). Its purity was determined to be better than 99% by HPLC. A stock solution (10^{-3} M) was prepared in distilled tetrahydrofuran (THF) and kept at −18°C. Experimental solutions were obtained by evaporating an aliquot of the stock solution to make a film that was dissolved in PBS. These were used without delay and renewed frequently.

This procedure was found to minimize aggregation and adsorption of DP on glass. The porphyrin solutions were handled in the dark to avoid any photobleaching.

Human low-density lipoproteins (LDL) were purchased from Calbiochem (San Diego, CA), or were prepared by sequential ultracentrifugation (Havel et al., 1955). The commercial material was conditioned in 0.15 M NaCl aqueous solution at pH 7.4 with 0.01% EDTA. The protein content of LDL solutions that we isolated was determined as described elsewhere (Peterson, 1977). The integrity of the LDL after storage and after mixing in the stopped-flow apparatus was assessed by acrylamide (7.5%) SDS-PAGE electrophoresis and Tris-glycine native agarose gel electrophoresis (1% agarose, 25 mM Tris base, 192 mM glycine, pH 8.4) according to protocols described elsewhere (Carr et al., 2000). When stored at 4°C, the stock solutions were found to be stable for about one month. Human serum albumin (HSA) essentially fatty acid-free was purchased from Sigma (St. Louis, MO), and stored at 4°C.

Measurements

Steady-state fluorescence measurements

Emission and excitation fluorescence spectra were recorded at 20°C using a SPEX spectrofluorimeter (Edison, NJ). Recording generally commenced 2 min after the preparation of the solutions under study. Data were fitted by using the Kaleidagraph software (Synergy Software, Reading, PA). The Levenberg-Marquard algorithm was used for nonlinear curve fitting. The Mathcad software (Mathsoft, Inc., Cambridge, MA) was used for numerical simulations of porphyrins binding to LDL.

Kinetic measurements

Measurements were performed at 20°C with the aid of an Applied Photophysics (Leatherhead, UK) stopped-flow apparatus with mixing time of 1.2 ms. The mixing ratio was 1:1. The excitation light provided by a 150 W xenon arc lamp was passed through a monochromator with slits generally set to give a bandwidth of 4.65 nm. Fluorescence emission was collected above 610 nm using a low-cut filter (Oriel, Palaiseau, France). The fluorescence signal was fed on a RISC workstation (Acorn Computers, Cambridge, UK) and analyzed using the software provided by the manufacturer.

Kinetic models

Interaction of porphyrin with LDL

Experimental results led us to consider two classes of porphyrins bound to LDL (defined as class P and class L). In a first approximation, we assume that binding of any molecule does not depend on the state of LDL occupancy. In other words, pseudo-first-order conditions are assumed. Also, the two binding classes are considered to be independent. Then,

$$P_F + \mathrm{LDL} \underset{k_{dP}}{\overset{k_{aP}}{\rightleftharpoons}} P_P$$

$$P_F + \mathrm{LDL} \underset{k_{dL}}{\overset{k_{aL}}{\rightleftharpoons}} P_L$$

where k_{aP} and k_{dP} are the association and dissociation rate constants for the class P sites, k_{aL} and k_{dL} are those for DP binding to the lipid phase (class L). P_F stands for the free porphyrin in aqueous solution.

The set of differential equations describing the system is:

$$dP_F/dt = k_{dL} \times P_L + k_{dP} \times P_P - (k'_{aL} + k'_{aP}) \times P_F \quad (1a)$$

$$dP_L/dt = k'_{aL} \times P_F - k_{dL} \times P_L \quad (1b)$$

$$dP_P/dt = k'_{aP} \times P_F - k_{dP} \times P_P \quad (1c)$$

where k'_{aP} and k'_{aL} are apparent association rate constants as functions of the LDL concentration according to:

$$k'_{aL} = k_{aL} \times \mathrm{LDL}$$

$$k'_{aP} = k_{aP} \times \mathrm{LDL}$$

The solution can be easily found by using Laplace transforms (Connors, 1990). With the initial conditions $P_{F(t=0)} = P_0$ and $P_{L(t=0)} = P_{P(t=0)} = 0$, the system is transformed into:

$$s \times \boldsymbol{P}_F - P_0 = -(k'_{aP} + k'_{aL}) \times \boldsymbol{P}_F + k_{dL} \times \boldsymbol{P}_L + k_{dP} \times \boldsymbol{P}_P$$

$$s \times \boldsymbol{P}_L = k'_{aL} \times \boldsymbol{P}_F - k_{dL} \times \boldsymbol{P}_L$$

$$s \times \boldsymbol{P}_P = k'_{aP} \times \boldsymbol{P}_F - k_{dP} \times \boldsymbol{P}_P$$

where s stands for the Laplace transform of the derivative function, and $\boldsymbol{P}_P$, $\boldsymbol{P}_L$, and $\boldsymbol{P}_F$ for the Laplace transforms of P_P, P_L, and P_F.

It follows:

$$\boldsymbol{P}_F = \frac{P_0 \times (s^2 + (k_{dP} + k_{dL}) \times s + k_{dP} \times k_{dL})}{s \times D}$$

$$\boldsymbol{P}_L = \frac{k'_{aL} \times P_0 \times (s + k_{dP})}{s \times D}$$

$$\boldsymbol{P}_P = \frac{k'_{aP} \times P_0 \times (s + k_{dL})}{s \times D}$$

where

$$D = s^2 + (k_{dP} + k_{dL} + k'_{aP} + k'_{aL}) \times s + k_{dP} \times k_{dL} + k'_{aL} \times k_{dP} + k'_{aP} \times k_{dL}$$

$$= (s + k_1) \times (s + k_2)$$

The inverse Laplace transforms yield the time dependence of P_F, P_L, or P_P concentrations. Biexponential functions with the same rate constants, k_1 and k_2, are obtained for the three species. These rate constants are the two roots (with sign inversion) of the polynomial D. The rate constants k_1 and k_2 (abbreviated $k_{1,2}$) are:

$$k_{1,2} = \tfrac{1}{2} \times [\Sigma k \pm \sqrt{(\Sigma k)^2 - 4 \times (k_{dP} \times k_{dL} + k'_{aL} \times k_{dP} + k'_{aP} \times k_{dL})}] \quad (2)$$

where

$$\Sigma k = k_{dP} + k'_{aP} + k_{dL} + k'_{aL}$$

For P_F, the Laplace transform method yields:

$$P_F = A_0 - A_1 \times \exp(-k_1 \times t) - A_2 \times \exp(-k_2 \times t) \quad (3)$$

where

$$A_0 = P_{F(t=0)} \times \frac{k_{dL} \times k_{dP}}{k_1 \times k_2} \quad (4)$$

The amplitudes of these two exponential terms are:

$$A_1 = P_{F(t=0)} \times \frac{k_1^2 - k_1(k_{dP} + k_{dL}) + k_{dP} \times k_{dL}}{k_1(k_2 - k_1)} \quad (5)$$

$$A_2 = P_{F(t=0)} \times \frac{k_2^2 - k_2(k_{dP} + k_{dL}) + k_{dP} \times k_{dL}}{k_2(k_1 - k_2)} \quad (6)$$

A biexponential signal would be expected. However, it reduces to a monoexponential when $k_{dP} \approx k_{dL}$, an approximation that appears to be valid for the present system (see Results). Indeed, substituting k'_{aP} and k'_{aL} by $k_{aP} \times [LDL]$ and $k_{aL} \times [LDL]$, and $k_{dP} \approx k_{dL}$ by k_d, we obtain:

$$k_1 \cong k_d \quad (7)$$

$$k_2 \cong (k_{aP} + k_{aL}) \times [LDL] + k_d \quad (8)$$

$$A_1 \cong P_{F(t=0)} \times \frac{(k_d^2 - 2k_d^2 + k_d^2)}{k_d \times (k_{aP} + k_{aL}) \times [LDL]} \quad (9)$$

$$A_2 \cong -P_{F(t=0)} \times \frac{(k_{aP} + k_{aL}) \times [LDL]}{k_d + (k_{aP} + k_{aL}) \times [LDL]} \quad (10)$$

However, the numerator of Eq. 9, giving the amplitude A_1, tends to zero. In addition, the presence of the LDL term only in the denominator further reduces the contribution of the first exponential at high lipoprotein concentration. The expressions describing the evolution of P_L and P_P have been calculated in the same way. They also involve the rate constants k_1 and k_2, and the amplitude of the first exponential terms tends to zero under the same conditions. As a consequence, when k_{dL} and k_{dP} approach one another, only the second exponential characterized by the rate constant k_2 is observed.

Numerical simulations using the Matcad software were carried out to estimate the range of validity for this approximation. Biexponential signals were generated with various k_{dL}/k_{dP} ratios and LDL concentrations according to Eqs. 2–6. They were then fitted by a single exponential, and residuals (signal minus curve fit) normalized to the total signal amplitude were calculated. When k_{dL} and k_{dP} differ by a factor of 2.6 (the value obtained from data analysis reported below), deviation cannot be distinguished from noise for LDL concentrations equal to or higher than 1×10^{-8} M (see Results). When the ratio is 5, deviation starts to be visible for a LDL concentration equal to 2×10^{-8} M. A ratio of 10 leads to deviation in the all range of LDL concentrations investigated.

Transfer of porphyrin from LDL to HSA

The transfer of porphyrin from preloaded LDL to HSA was assumed to occur via the aqueous phase according to the following equilibria:

$$P_P \underset{k'_{aP}}{\overset{k_{dP}}{\rightleftarrows}} P_F \underset{k_{dH}}{\overset{k'_{aH}}{\rightleftarrows}} P_H$$

$$k_{dL} \uparrow\downarrow k'_{aL}$$

$$P_L$$

where k'_{aH} is the pseudo-first-order association rate constant and k_{dH} the dissociation rate constant relative to porphyrin-HSA binding. It was further assumed that under our experimental conditions, the interactions of the free porphyrin with LDL and albumin are pseudo-first-order processes. Then, the kinetics of the transfer process is described by the system of equations:

$$dP_F/dt = k_{dL} \times P_L + k_{dP} \times P_P + k_{dH} \times P_H - (k'_{aL} + k'_{aP} + k'_{aH}) \times P_F \quad (11a)$$

$$dP_L/dt = k'_{aL} \times P_F - k_{dL} \times P_L \quad (11b)$$

$$dP_P/dt = k'_{aP} \times P_F - k_{dP} \times P_P \quad (11c)$$

$$dP_H/dt = k'_{aH} \times P_F - k_{dH} \times P_H \quad (11d)$$

The solution of this system involves exponential terms with complex analytical expressions. However, owing to the large LDL and HSA concentrations used experimentally, a considerable simplification can be obtained. Indeed, the rate constants of the association of DP to albumin or LDL are much larger than the dissociation constants. Consequently, the steady-state approximation of Bodenstein holds, i.e., $dP_F/dt = 0$ (except during a short initial period). Thus, we can express P_F as a function of P_P, P_L, and P_H. Moreover, considering that in our experiments [HSA] $\gg$ [LDL], the rate constant of the association of DP to albumin ($k'_{aH} = k_{aH} \times [HSA]$) is much larger than constants of the association with LDL. Then,

$$\frac{dP_P}{dt} = \left(\frac{k_{aP} \times k_{dP}}{k_{aH}} - k_{dP}\right) \times P_P + \frac{k_{aP} \times k_{dL}}{k_{aH}} \times P_L + \frac{k_{aP} \times k_{dH}}{k_{aH}} \times P_H$$

$$\frac{dP_L}{dt} = \frac{k_{aL} \times k_{dP}}{k_{aH}} \times P_P + \left(\frac{k_{aL} \times k_{dL}}{k_{aH}} - k_{dL}\right) \times P_L + \frac{k_{aL} \times k_{dH}}{k_{aH}} \times P_H$$

$$\frac{dP_H}{dt} = k_{dP} \times P_P + k_{dL} \times P_L$$

By using Laplace transforms with the initial conditions $P_{F(t=0)} = P_{H(t=0)} = 0$ and $P_{L(t=0)} = P_{L0}$, $P_{P(t=0)} = P_{P0}$ and neglecting terms that become small when [HSA] $\gg$ [LDL], we obtain:

$$\boldsymbol{P}_P = \frac{\left(\frac{k_{aP} \times k_{dL}}{k_{aH}} \times s\right) \times P_{L0} + (s^2 + k_{dL} \times s) \times P_{P0}}{s \times D}$$

$$\boldsymbol{P}_L = \frac{\left(\frac{k_{aL} \times k_{dP}}{k_{aH}} \times s\right) \times P_{P0} + (s^2 + k_{dP} \times s) \times P_{L0}}{s \times D}$$

$$\boldsymbol{P}_H = \frac{\left\{\begin{array}{l}\left[k_{dP} \times s + \left(k_{dP} \times k_{dL} + \frac{k_{dL} \times k_{aL} \times k_{dP}}{k_{aH}}\right)\right] \times P_{P0} \\ + \left[k_{dL} \times s + \left(k_{dP} \times k_{dL} + \frac{k_{dL} \times k_{aL} \times k_{dP}}{k_{aH}}\right)\right] \times P_{L0}\end{array}\right\}}{s \times D}$$

with

$$D = s^2 + (k_{dL} + k_{dP}) \times s + k_{dL} \times k_{dP}$$
$$= (s + k_{dL}) \times (s + k_{dP}) \quad (12)$$

The inverse Laplace transforms give the expressions describing the evolution of P_H, P_L, and P_P as a function of time. Each expression consists of the sum of one constant and two exponential terms. The rate constants k_1 and k_2 are the roots (with sign inversion) of Eq. 12 for $D = 0$.

$$k_1 = k_{dP} \quad (13)$$

$$k_2 = k_{dL} \quad (14)$$

For each of the exponentials noted 1 and 2, the contributions of the various forms of the porphyrin (noted H, P, L) to the amplitudes (A) are:

$$A_{H,1} = \frac{\left(k_{dL} - k_{dP} + \frac{k_{aL} \times k_{dL}}{k_{aH}}\right) \times P_{P0} + \frac{k_{aP} \times k_{dL}}{k_{aH}} \times P_{L0}}{k_{dL} - k_{dP}}$$

$$A_{H,2} = \frac{\frac{k_{aL} \times k_{dP}}{k_{aH}} \times P_{P0} + \left(k_{dP} - k_{dL} + \frac{k_{aP} \times k_{dP}}{k_{aH}}\right) \times P_{L0}}{k_{dP} - k_{dL}}$$

$$A_{P,1} = \frac{(k_{dP} - k_{dL}) \times P_{P0} + \frac{k_{aP} \times k_{dL}}{k_{aH}} \times P_{L0}}{k_{dL} - k_{dP}}$$

$$A_{P,2} = \frac{k_{aP} \times k_{dL}}{k_{aH} \times (k_{dP} - k_{dL})} \times P_{L0}$$

$$A_{L,1} = \frac{k_{aL} \times k_{dP}}{k_{aH} \times (k_{dL} - k_{dP})} \times P_{P0}$$

$$A_{L,2} = \frac{(k_{dL} - k_{dP}) \times P_{L0} + \frac{k_{aL} \times k_{dP}}{k_{aH}} \times P_{P0}}{k_{dP} - k_{dL}}$$

It can be easily shown that the contributions of each form to the two exponential terms are similar, even when the values of k_{dP} and k_{dL} are close.

RESULTS

Steady-state measurements

Fluorescence spectra

The fluorescence emission spectra of DP in buffer, bound to LDL or HSA, are shown in Fig. 2. The concentrations of LDL (10^{-7} M) or HSA (5×10^{-6} M) were sufficient to ensure total porphyrin binding (see equilibrium constants below). The excitation wavelength was set at 396 nm, the maximum of the excitation spectrum of DP bound to LDL. The main emission band is shifted from 609 nm in PBS to 621 nm and 623 nm when the porphyrin is bound to LDL and HSA, respectively. Albumin and LDL do not fluoresce in this spectral range. As shown in Fig. 2, the emission and excitation spectra appear to be different enough to easily monitor changes in the porphyrin environment. A specific peak around 280 nm can be noted in the excitation spectrum of DP bound to LDL. No fluorescence excitation band below 300 nm is observed for free deuteroporphyrin.

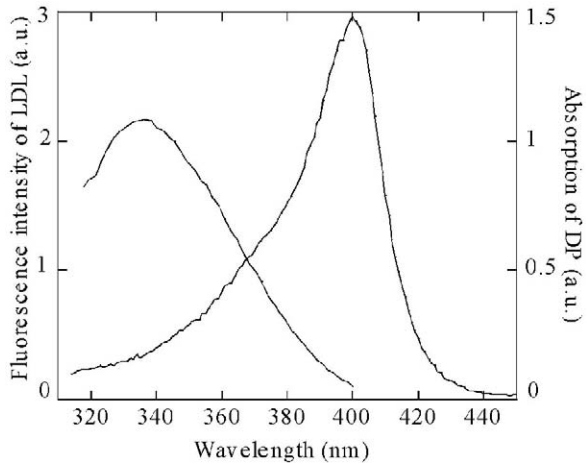

FIGURE 3 Fluorescence emission spectrum of LDL in the absence of deuteroporphyrin (excitation 280 nm, *left scale*) and absorption spectrum of LDL-bound deuteroporphyrin corrected for LDL absorption (*right scale*). The overlap of spectra demonstrates the feasibility of fluorescence resonance energy transfer (FRET).

Upon excitation at 280 nm, LDL displays an intrinsic fluorescence emission band around 330 nm due to tryptophan residues. As shown in Fig. 3, there is a significant overlap between the emission spectrum of LDL and the absorption spectrum of DP. Then, fluorescence resonance energy transfer (FRET) from tryptophan residues of apoB100 to DP is thus possible. According to Förster's equation, the efficiency of the transfer varies as the inverse sixth power of the distance between the two partners and is therefore strongly distance-dependent. The Förster's distance that corresponds to half of the energy transferred has been estimated to be ~1.7 nm for a related porphyrin-tryptophan couple (Moan et al., 1985). Hence, porphyrin molecules close to tryptophan residues, i.e., bound to apoprotein B100 or at the frontier between the protein and lipids can be characterized by FRET.

Quantification of porphyrin binding to LDL by tryptophan fluorescence quenching

The peak around 280 nm in the excitation spectrum of DP bound to LDL corresponds to the excitation maximum of tyrosine/tryptophan fluorescence indicating FRET. This gives a clear indication of the existence of porphyrin sites close to the protein. Concomitantly, as shown in Fig. 4 *A*, the intrinsic fluorescence of apoprotein B100 is quenched upon binding of porphyrin in a concentration-dependent way. This first class of sites will be denoted as class P,

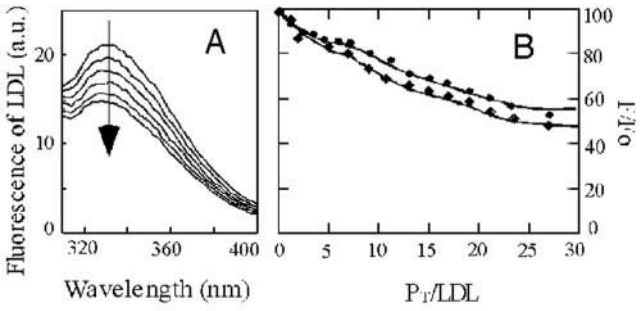

FIGURE 4 Quenching of LDL intrinsic fluorescence (excitation wavelength: 280 nm) upon deuteroporphyrin binding. (*A*) Fluorescence spectra of LDL (4×10^{-8} M) as a function of DP concentration; P_T/LDL: 0, 5, 7, 11, 15, 19 in the arrow direction; (*B*) relative fluorescence intensity (F/F_0, %) at 330 nm vs. P_T/LDL. (◆) [LDL] = 6×10^{-8} M; (●) [LDL] = 4×10^{-8} M. Fluorescence intensities for $P_T = 0$ (F_0) are normalized to 100%.

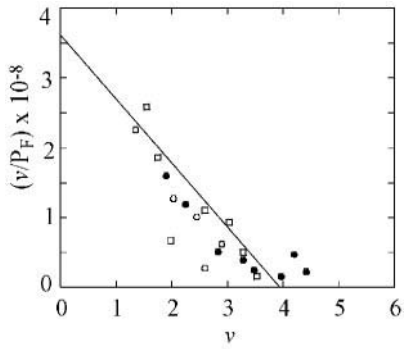

FIGURE 5 Quantification of binding of deuteroporphyrin to LDL followed by changes of LDL intrinsic fluorescence at 330 nm (excitation wavelength 280 nm). The Scatchard plot is obtained from data computed according to the Halfman and Nishida method. The three symbols correspond to LDL from various origins; (●, ○) home-made LDL; (□) commercial LDL.

hereafter. A linear relation between FRET efficiency and the number of porphyrins bound to LDL is not expected, however. Indeed, for each binding site, the efficiency will depend on the distance and relative orientation of the porphyrin and the nearest tryptophan residues. Hence, we used the method developed by Nishida (Halfman and Nishida, 1972) as follows. By definition, for any LDL concentration,

$$P_F = \text{LDL} \times \left(\frac{P_T}{\text{LDL}} - \nu \right) \tag{15}$$

where ν is the number of porphyrin molecules bound per LDL molecule and P_T the total porphyrin concentration. The Nishida method is based on the existence of pairs of P_T and LDL concentrations yielding the same value of ν. Then, for two pairs noted *a* and *b* it follows from the direct relation between P_F and ν and from Eq. 15:

$$\nu = \frac{(P_{Ta}/\text{LDL}_a) - \dfrac{\text{LDL}_b}{\text{LDL}_a}(P_{Tb}/\text{LDL}_b)}{1 - \dfrac{\text{LDL}_b}{\text{LDL}_a}} \tag{16}$$

$$P_F = \frac{\text{LDL}_a \times \text{LDL}_b}{\text{LDL}_a - \text{LDL}_b}\left[(P_{Tb}/\text{LDL}_b) - (P_{Ta}/\text{LDL}_a)\right] \tag{17}$$

It is further assumed that a value of ν corresponds to a unique value of the relative change of a protein property. Here, this property is the tryptophan fluorescence expressed as the ratio F/F_0, where F and F_0 are the fluorescence intensities in the presence and absence of DP, respectively. The quenching efficiency was measured, for two close concentrations of LDL, as a function of the total DP concentration (Fig. 4 *B*). The decrease of F/F_0 upon addition of relatively low amounts of DP indicates the presence of high-affinity sites. Pairs of P_T and LDL concentrations yielding the same value of F/F_0 were selected, and the values of ν and P_F were derived according to Eqs. 16 and 17. Then, results were plotted according to the Scatchard method:

$$\frac{\nu}{P_F} = nK_i - \nu K_i \tag{18}$$

As shown in Fig. 5, the Scatchard plot led to the identification of about four sites. The mean intrinsic affinity per site, K_{pi}, was found to be 9×10^7 M^{-1}. It can be noted that similar results were obtained with commercial and laboratory-made LDL.

Porphyrin fluorescence changes upon binding to LDL

As shown in Fig. 2, binding of porphyrin to LDL leads to important fluorescence modifications. The emission spectrum is characteristic of that for porphyrin in a lipidic environment (Brault et al., 1986; Kuzelova and Brault, 1994). Preliminary fluorescence studies with increasing lipoprotein concentrations showed that the binding capacity of LDL greatly exceeds that of the four sites identified above. Nevertheless, when the LDL concentration was large enough to bind all the porphyrin molecules, emission and excitation spectra of DP did not depend on the ratio DP/LDL. Thus, the fluorescence characteristics of DP bound to different locations are similar. Overall binding can be monitored by changes in the porphyrin fluorescence without distinguishing sites.

In the range of concentrations used, the fluorescence of any solution is a linear combination of the fluorescence of the individual porphyrin components at a given wavelength. We considered the porphyrin free in solution (P_F) and the porphyrin bound to LDL (P_B) with main peaks at 609 nm

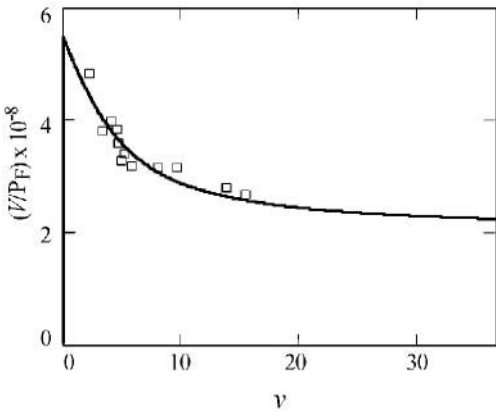

FIGURE 6 Quantification of binding of deuteroporphyrin to LDL followed by changes of DP fluorescence at 621 nm (excitation wavelength 396 nm). The curve is computed according to Eq. 22.

and 621 nm, respectively. We can write for these two wavelengths:

$$F_{609} = f_{B,609} \times P_B + f_{F,609} \times P_F \quad (19)$$

$$F_{621} = f_{B,621} \times P_B + f_{F,621} \times P_F \quad (20)$$

The proportionality factors $f_{F,609}$, $f_{F,621}$, $f_{B,609}$, and $f_{B,621}$ were derived from calibration experiments on free DP and LDL-bound DP (LDL in excess) at the two wavelengths, respectively. Then, the concentrations P_F and P_B were calculated from the above set of linear equations for any solution of intermediate composition. The number of porphyrin molecules bound per LDL molecule, ν, was calculated accordingly. As shown in Fig. 6, the Scatchard plot, ν/P_F vs. ν, thus obtained shows a marked curvature indicating that more than one class of sites is involved.

The overall binding capacity of LDL has been estimated by recording the fluorescence emission spectra of solutions containing a fixed lipoprotein amount and increasing porphyrin concentrations. Bound and free DP concentrations were calculated according to Eqs. 19 and 20. The bound DP concentration increased, reaching a plateau at ~55 porphyrin molecules per LDL, which corresponds to lipoprotein saturation (data not shown).

Overall binding scheme

The number of class P sites being limited to about four, other LDL compartments including the outer phospholipid layer and the inner core should be involved (class L binding sites). The overall binding would then be described by:

$$\frac{\nu}{P_F} = \frac{n_P \times K_{Pi}}{1 + P_F \times K_{Pi}} + \frac{n_L \times K_{Li}}{1 + P_F \times K_{Li}} \quad (21)$$

where K_{Pi}, K_{Li}, n_P, and n_L are the intrinsic microscopic affinity constants and the corresponding number of sites for the P and L classes, respectively.

In keeping with earlier studies (Beltramini et al., 1987), the second interaction type would be better viewed as a partition of DP between the bulk aqueous phase and the lipidic phase of LDL (see Fig. 1). The above equation can be rewritten using the same formalism but with the following assumption: the porphyrin can reach a large number of lipidic "sites" possessing a low intrinsic affinity ($P_F \times K_{Li} \ll 1$). It follows that:

$$\frac{n_L \times K_{Li}}{1 + P_F \times K_{Li}} \rightarrow n_L \times K_{Li}$$

We can define a macroscopic affinity constant, $K_L = n_L \times K_{Li}$. Then,

$$\frac{\nu}{P_F} = \frac{n_P \times K_{Pi}}{1 + P_F \times K_{Pi}} + K_L \quad (22)$$

Experimental data have been fitted according to Eq. 22 by nonlinear regression analysis, the overall affinity constant being fixed at 5.8×10^8 M^{-1}, in agreement with results presented below. The values of K_{Pi}, n_p, and K_L thus derived are given in Table 1. The theoretical fit is shown in Fig. 6 as a Scatchard plot.

The association of DP with LDL was also studied by varying the LDL concentration for a constant porphyrin concentration. Analysis of fluorescence data according to the method previously used for liposomes (Brault et al., 1986; Kuzelova and Brault, 1994) led to an overall association constant of $(5.8 \pm 1.2) \times 10^8$ M^{-1}.

Kinetic measurements

Association of deuteroporphyrin and LDL

To follow the association of DP with LDL, different porphyrin solutions were mixed with a series of LDL solutions in the stopped-flow apparatus and fluorescence changes were recorded versus time. The porphyrin concentrations

TABLE 1 Values of equilibrium and rate constants of association of deuteroporphyrin with the low-density lipoproteins

	Equilibrium Constants			Rate Constants				
n_P	K_{Pi}	K_P	K_L	k_{aPi}	k_{aP}	k_{dP}	k_{aL}	k_{dL}
	9×10^7 M^{-1}*	3.6×10^8 M^{-1}*		5×10^8 $M^{-1}s^{-1}$	2×10^9 $M^{-1}s^{-1}$	$5.8s^{-1}$	3×10^9 $M^{-1}s^{-1}$	$15s^{-1}$
4*†	8.75×10^7 M^{-1}†	3.5×10^8 M^{-1}†	2×10^8 M^{-1}†					

*Values calculated from the Scatchard plots obtained by following the quenching of lipoprotein intrinsic fluorescence.
†Values calculated from the Scatchard plots obtained by following the porphyrin fluorescence.

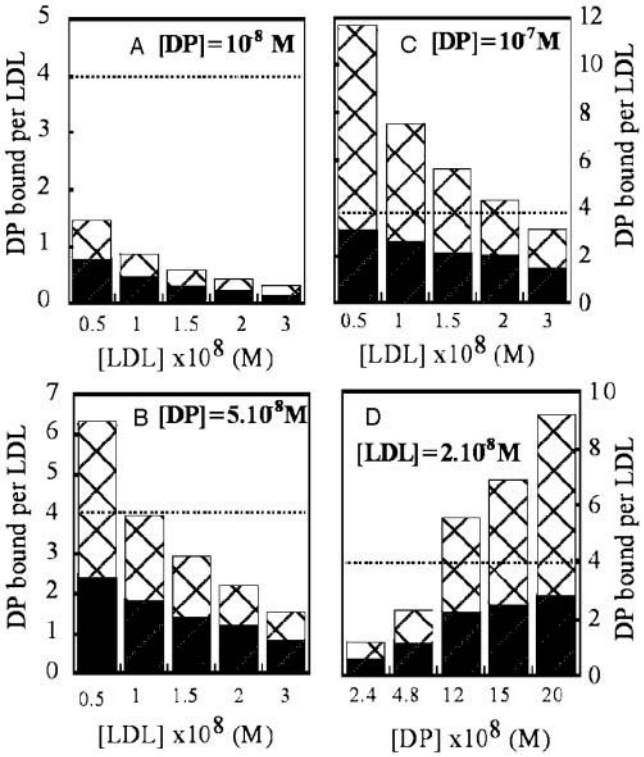

FIGURE 7 Stacked column representation of the number of porphyrins per LDL at equilibrium under various experimental conditions. The numbers of porphyrins bound to class P sites and incorporated into the LDL lipid phase are shown in black and grid areas, respectively. The number of accessible class P sites is indicated by a dashed line. The overall binding capacity of LDL is ~55 porphyrin molecules. The values have been computed using the equilibrium constants reported in Table 1.

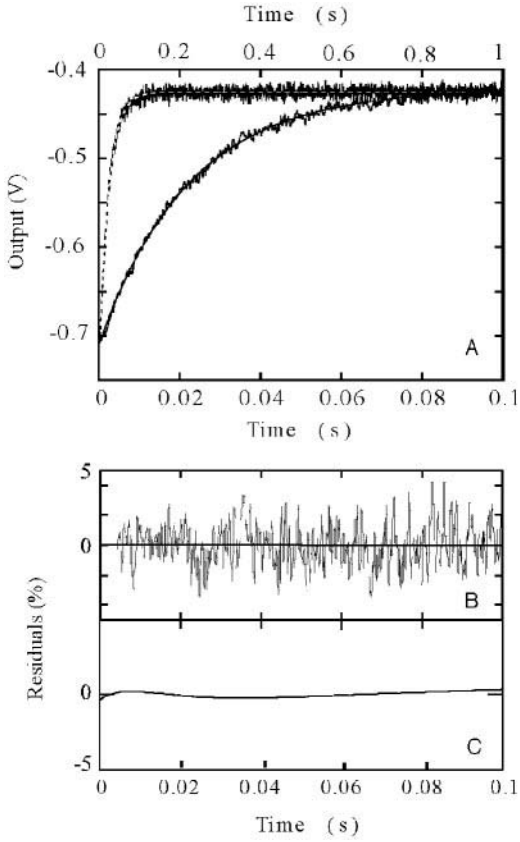

FIGURE 8 Kinetics of binding of deuteroporphyrin to LDL. (*A*) Fluorescence intensity changes recorded upon mixing LDL (final concentration: 2×10^{-8} M) with deuteroporphyrin (1×10^{-8} M); excitation wavelength, 405 nm. Signals recorded by using two time scales are shown. The best monoexponential fit leading to the observed pseudo-first-order rate constant k^{obs} is superimposed on the signals. (*B*) Normalized residuals of the monoexponential fit of experimental data. (*C*) Normalized residuals of the monoexponential fit of a biexponential signal simulated using the rate constant values given in Table 1.

were 1×10^{-8}, 5×10^{-8}, and 1×10^{-7} M, and those of LDL 5×10^{-9}, 1×10^{-8}, 1.5×10^{-8}, 2×10^{-8}, and 3×10^{-8} M after mixing. The number of porphyrin molecules bound per LDL at sites of class P and in the lipid moiety after completion of equilibria have been calculated by using the equilibrium constants determined above. The values are given in Fig. 7, *A–C*.

A typical fluorescence signal is shown in Fig. 8 *A* for the more diluted porphyrin solution. The changes were found to be fairly fast and the signal nicely fitted by a monoexponential (see Fig. 8 *B*). No other change was recorded over seconds in stopped-flow experiments or over at least 2 h when solutions were mixed manually and fluorescence recorded by using a conventional spectrofluorimeter. The signals for the other sets of concentrations were very similar, except the quality of the monoexponential fit was less for the highest porphyrin/LDL ratios. At the lower porphyrin concentration, the sites of class P are far from being saturated. On average, less than one site among four is occupied. In the same way, the binding capacity of the lipid phase greatly exceeds the number of bound porphyrins. In these conditions, the interactions of DP with LDL are considered as pseudo-first-order processes.

According to the theoretical model presented in the previous section, in the most general case, the evolution of the concentration of P_F, P_P, and P_L, should be described by a biexponential under pseudo-first-order conditions. However, when the dissociation rate constants for the two classes of sites are close ($k_{dP} \approx k_{dL} \approx k_d$), the amplitude of the slower component vanishes. Even if these rate constants are not equal, it would be very difficult to distinguish a small slow component from the large fast signal. Numerical simulations (see above section) show that the dissociation rate constants must differ by a factor of at least five to yield significant deviation from monoexponential fit. An example of simulation is given in Fig. 8 *C*. The rate constants (k_{dP} = 5.8, k_{dL} = 15) determined by the method of transfer to albumin described below were used. The relative amplitude of the slow exponential was found to be only 2.3% of the total. The comparison of the residuals obtained from the fit of data (Fig. 8 *B*) and from simulation (Fig. 8 *C*) clearly

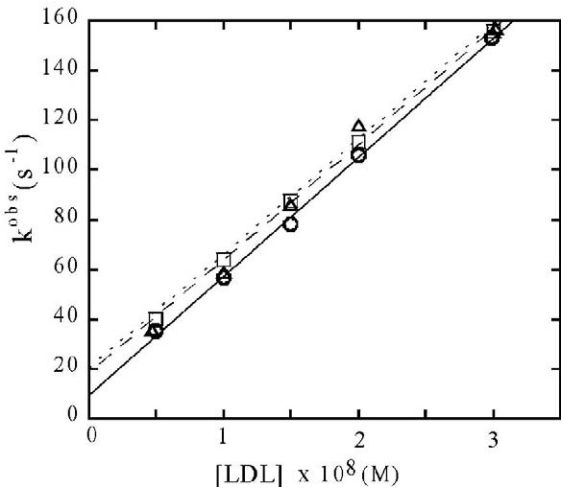

FIGURE 9 Plot of the observed pseudo-first-order rate constant (k^{obs}) versus LDL concentration. The porphyrin concentrations are (○) 1×10^{-8} M, (□) 5×10^{-8} M, and (△) 1×10^{-7} M.

shows that the deviation introduced by the monoexponential approximation cannot be distinguished from the experimental noise. Only one exponential is observed experimentally. Thus, results were analyzed to a first approximation as a pseudo-first-order single process leading to an observed rate constant k^{obs} that corresponds to k_2 in our theoretical model.

Data shown in Fig. 9 are well-fitted by straight lines according to,

$$k^{obs} = k_a^{obs} \times [LDL] + k_d^{obs} \quad (23)$$

Although all the values of k^{obs} are depicted on the plot, only those corresponding to <10% of overall site occupancy were retained for the linear fit to obey pseudo-first-order approximation. The apparent association rate constant k_a^{obs} was found to be fairly independent on experimental conditions, with a value of $k_a^{obs} = (4.65 \pm 0.10) \times 10^9\ M^{-1}\ s^{-1}$. The intercept of the linear fit, k_d^{obs}, ranges between 9 and 21 s^{-1}. The highest value was found for the highest porphyrin concentration, i.e., when the number of molecules incorporated into the lipid phase greatly exceeds that of porphyrins bound to class P sites (see Fig. 7, *A–C*). This suggests that k_{dL} might be somewhat larger than k_{dP}.

Transfer of deuteroporphyrin from LDL to albumin

To better approximate the values of k_{dP} and k_{dL}, the transfer of the porphyrin from preloaded LDL to albumin in excess was investigated. In previous studies, this approach was found to be quite efficient to determine exit rate constants of porphyrins from liposomes (Kuzelova and Brault, 1994; Maman and Brault, 1998).

According to our theoretical model, the transfer from LDL would be described by two exponentials under two limiting conditions. First, the concentration of LDL must be sufficient to bind most of the porphyrin molecules. Second, a complete porphyrin transfer must be ensured by using albumin in large excess ($k'_{aH} = k_{aH} \times [HSA] \gg k'_{aP}, k'_{aL}$). Then, the exponential factors give k_{dL} and k_{dP} directly. Remarkably, the amplitudes of the two exponentials are of the same order of magnitude, contrary to observations for the direct interaction of the porphyrin with LDL. Thus, fitting is greatly facilitated.

Experimentally, solutions of porphyrin were first incubated with LDL for 2 h at room temperature. The repartition of porphyrins molecules between the two binding classes is indicated in Fig. 7 *D*. They were then mixed in the stopped-flow apparatus with solutions of albumin in large excess (10^{-4} M after mixing). The transfer was followed by fluorescence (see Fig. 2 for spectra) with the excitation wavelength set at 396 nm, to yield the largest signal. A typical trace is shown in Fig. 10 *A*. Clearly, the signal is better fitted by two exponentials with almost equal amplitudes, as predicted by our model (see Fig. 10, *B* and *C*). As expected from the spectra shown in Fig. 2, when excitation was set at 410 nm the fluorescence increased, but the rate constants and the relative amplitudes of the two phases remained unchanged. Rate constants of ~5 s^{-1} and ~15 s^{-1} were obtained from the fits. On the basis of the results for the interaction of DP with LDL described above, the lower value was assigned to k_{dP}.

The dissociation rate constants being known, it is possible to calculate the association rate constants from the equilibrium constants derived independently from the Scatchard plots, assuming that $K = k_a/k_d$. Values of the rate constants are summarized in Table 1.

As shown in Fig. 10 *D*, a slower phase with a rate constant around 0.1 s^{-1} was also detected. Its direction was always opposite to that of the main signal, whatever the excitation wavelength. The inversion of the signal was observed at the same excitation wavelength (around 406 nm) for the fast and the slow phases. However, the amplitude of the slow phase never exceeded ~10% of the total signal.

To further sustain the above models and the approximations made to analyze data, the kinetics of the interactions of the porphyrin with LDL and the kinetics of the transfer of the porphyrin from LDL to albumin were simulated by using the Mathcad mathematical software. The program involves the original sets of differential equations 1a–c and 11a–d without any assumptions and does not presuppose pseudo-first-order conditions. The rate constants for albumin were taken as $k_{aH} = 6.75 \times 10^7\ M^{-1}\ s^{-1}$ and $k_{dH} = 3.5\ s^{-1}$ (Kuzelova and Brault, 1994). The known initial concentrations and estimates for the rate constants k_{aP}, k_{aL}, k_{dP}, and k_{dL} were entered into the program. The simulated curves were fitted by exponentials in the same way as experimental data. The values of the rate constants k_{aP}, k_{aL}, k_{dP}, and k_{dL} were adjusted so that the exponential factors obtained from the fit of experimental traces and simulated

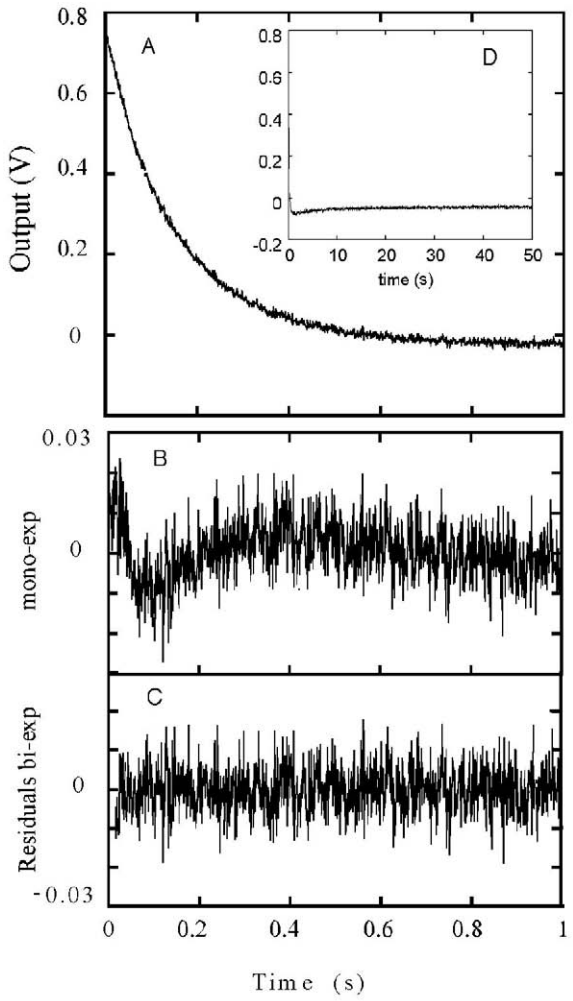

FIGURE 10 Kinetics of the transfer of deuteroporphyrin from LDL to HSA. (*A*) Fluorescence intensity changes recorded upon mixing LDL preloaded with porphyrin and HSA. Final concentrations: DP = 1.5×10^{-7} M; LDL = 2×10^{-8} M; HSA = 1×10^{-4} M. Excitation wavelength 396 nm. (*B*) Residuals from the best monoexponential fit. The sum of the squared differences between experimental data and the curve fit (χ^2) is 0.093339. (*C*) Residual from the best biexponential fit. χ^2 is reduced to 0.078282. (*D*) Fluorescence intensity changes recorded over longer time.

curves were the same. The values of k_{aP}, k_{aL}, k_{dP}, and k_{dL} that were retained allowed adequate simulations of all the kinetics, including the transfer to albumin. These values were found to be similar to those given in Table 1. The validity of the approximations made and the fact that k_{dL} is higher than k_{dP} were confirmed. However, simulations did not predict a third slow phase. Thus, the aqueous phase transfer model accounts for the fast steps but does not explain the slower step. That will be discussed below.

DISCUSSION

The quenching of the intrinsic apoprotein fluorescence and changes in the fluorescence of porphyrins upon interaction with LDL made it possible to observe and characterize two types of binding sites. The first set comprises about four sites and involves quenching of tryptophan fluorescence. The second set is not likely to involve discrete sites, although saturation is observed when ~50 porphyrin molecules are incorporated. It could be better viewed as a solubilization of the porphyrin in the LDL lipid phase.

The first set could involve sites localized at the protein surface, or more deeply at the interface between the apoprotein and the LDL lipid phase. In fact, the apoprotein emission spectrum is peaking at 330 nm, a value typical of tryptophan in a nonpolar environment (Lakowicz, 1983), suggesting interactions with the LDL lipid phase. Also, the fluorescence properties of deuteroporphyrin bound to class P sites are very similar to those presented by the porphyrin in a lipidic environment. This suggests that the first class of sites involves the lipid protein-interface.

Further insight into the nature of binding processes of DP to LDL can be obtained from analysis of kinetics. The second-order rate constants for the association of the porphyrin with LDL can be compared to that of a process limited by diffusion of these species in solution. The theoretical limit is given by:

$$k_d = 4\pi(R_{LDL} + R_P)(D_{LDL} + D_P)N \qquad (24)$$

where R_{LDL} and R_P are the radii of the LDL and porphyrin, and D_{LDL} and D_P are the diffusion coefficients of LDL and porphyrin, respectively (Connors, 1990); N is Avogadro's number. The diffusion coefficient of porphyrin was estimated to be $(2.4 \pm 1.0) \times 10^{-10}$ m^2/s (Vever-Bizet and Brault, 1993). The diffusion of LDL is much slower, with a D_{LDL} value of 2×10^{-11} m^2/s (Lee and Alaupovic, 1974). The radius of LDL is taken as 11×10^{-9} m (Schumaker et al., 1994; Segrest et al., 2001). The radius of porphyrin is 5×10^{-10} m. By using the above equation with appropriate unit conversion, the diffusion limit is calculated to be 2.3×10^{10} M^{-1} s^{-1}. However, phospholipids cover only half the LDL surface (Segrest et al., 2001), reducing the theoretical limit to $\sim 1.2 \times 10^{10}$ M^{-1} s^{-1}. With a rate constant of 3×10^9 M^{-1} s^{-1}, the association of DP to the LDL lipid phase approaches the diffusion limit. In previous experiments with unilamellar vesicles made of pure phospholipids in the fluid state, this limit was reached. The rate constant for the binding to class P sites, 5×10^8 M^{-1} s^{-1}, is ~50 times lower than the diffusion limit. In fact, this decrease is less than expected if we consider that binding involves discrete sites with a size comparable to that of the porphyrin. At least, the reduction should correspond to the ratio between the surfaces of LDL and porphyrin, i.e., $\sim 6 \times 10^3$. Binding of the porphyrin to some larger regions at the boundary between the apoprotein and the lipid phase appears more likely. The apoprotein is organized around the particle and displays alternating β-sheets and amphipathic α-helices. The β-sheets are in contact with irreversibly associated lipids likely involving cholesterol esters or-

dered in a smectic phase. The amphipathic α-helices are associated with the surface phospholipids. Except for the N-terminal globular domain, a large part of the apoprotein lies in a hydrophobic environment offering possible binding areas (Segrest et al., 2001).

The efficiency of lipoproteins as photosensitizer carriers would be significantly increased if the sensitizer can be solubilized within the lipid core. Such an incorporation could be possible, even at neutral pH, for dicarboxylic porphyrins. Indeed, the pK values of the carboxylic groups are strongly shifted toward higher values upon interactions with phospholipids (Brault et al., 1986). The association kinetics of deuteroporphyrin with LDL can be described as single exponentials. No evidence was found for slower processes in stopped-flow experiments or upon conventional fluorescence measurements after manual mixing. It must be noted that the overall association constant $K = (5.8 \pm 1.2) \times 10^8\ M^{-1}$, measured at equilibrium, is close to the ratio k_a^{obs}/k_d^{obs}, giving a value between 5.2×10^8 and $2.2 \times 10^8\ M^{-1}$ as derived from the plots shown in Fig. 9. It is expected that the population of the lipidic inner core of LDL would be slower and could be distinguished kinetically. Thus, it is very likely that the incorporation of deuteroporphyrin into LDL is limited to the outer layer of LDL and sites close to the interface with the apoprotein.

This view is further supported by comparison of the value of the affinity of deuterporphyrin for the lipidic components of LDL and that for unilamellar lipidic vesicles. Comparison can be made on the basis of the number of phospholipids molecules on the outer layer of LDL ($\sim$800). The affinity constant per phospholipid is calculated to be $2.5 \times 10^5\ M^{-1}$, a value of the same order of magnitude as the value measured for unilamellar vesicles (Kuzelova and Brault, 1994; Maman and Brault, 1998). We did not find any increase of affinity that could indicate a significant solubilization of the porphyrin in the LDL lipidic core. Nevertheless, the affinity constant is fairly high, illustrating the efficacy of LDL to carry lipophilic compounds. For comparison, the affinity of meso-tetrakis(*p*-sulfonatophenyl)porphyrin, a hydrophilic photosensitizer, for albumin is around $1 \times 10^6\ M^{-1}$ (Andrade and Costa, 2002).

The transfer of deuteroporphyrin to albumin gave further information on the exit rate constants from the two classes of sites of LDL. The third slow phase with a small amplitude and a direction always opposite to that of the fast components was unexpected. Numerical simulations show that forth and back transfer from LDL to albumin could take place with an appropriate combination of rate constants. This process would arise if the exit rates for the two classes of sites are very different, leading to a slow redistribution of the porphyrin between LDL sites and HSA, but these sets of rate constants would also predict biexponential kinetics for the association of DP with LDL, which is not observed. The slow phase might also be due to interactions between albumin and LDL, a phenomenon that was suggested elsewhere (Ho et al., 1996) and that could also take place with liposomes (Galantai et al., 2000). In any way, this phenomenon represents $<10\%$ of the observed signal. A detailed analysis appears to be beyond the scope of the present study.

CONCLUSIONS

The present results give new insight into the role of LDL particles as carriers of hydrophobic porphyrins. First, the binding of the porphyrin to the apoprotein appears to be limited and is not likely to involve the outer domain of the apoprotein. As a matter of fact, the recognition of LDL by their cellular receptor has been shown to be unaltered upon binding of related porphyrins (Candide et al., 1986; de Smidt et al., 1993). Second, the interactions of the porphyrin with LDL particles are very fast compared to the rate of lipopotein transport in biological fluids. At plasmatic physiological LDL concentrations (7×10^{-6} M), the half-time for association is $\sim 2 \times 10^{-5}$ s and that for dissociation between 0.05 and 0.12 s. Therefore, the transport of porphyrins by LDL must be considered as a dynamic process. The distribution of the porphyrin among various carriers will modify readily in response to a change in environment, in particular that provided by the interstitial liquid of tumors (Cunderlikova et al., 2000). Considering the rapidity of the processes, exchange might even occur while the LDL particles are bound to their cellular receptor. The knowledge and the control of the dynamics of photosensitizer LDL association, which can extend to the design of covalent LDL conjugates (Schmidt-Erfurth et al., 1997), are expected to contribute significantly to the improvement of photosensitizer targeting via the lipoprotein receptor pathway.

We are indebted to Pr. R. Santus for his interest in this work and helpful discussion. We are grateful to Josiane Haigle and François Guillonneau for their help in LDL handling and electrophoresis experiments. We thank Dr. L. K. Patterson for helpful suggestions in the preparation of the manuscript.

REFERENCES

Andrade, S. M., and S. M. Costa. 2002. Spectroscopic studies on the interaction of a water-soluble porphyrin and two drug carrier proteins. *Biophys. J.* 82:1607–1619.

Beltramini, M., P. A. Firey, F. Ricchelli, M. A. Rodgers, and G. Jori. 1987. Steady-state and time-resolved spectroscopic studies on the hematoporphyrin-lipoprotein complex. *Biochemistry.* 26:6852–6858.

Biade, S., J. C. Maziere, L. Mora, R. Santus, C. Maziere, M. Auclair, P. Morliere, and L. Dubertret. 1993. Lovastatin potentiates the photocytotoxic effect of photofrin II delivered to HT29 human colonic adenocarcinoma cells by low density lipoprotein. *Photochem. Photobiol.* 57: 371–375.

Boyle, R. W., and D. Dolphin. 1996. Structure and biodistribution relationships of photodynamic sensitizers. *Photochem. Photobiol.* 64: 469–485.

Brault, D., C. Vever-Bizet, and T. Le Doan. 1986. Spectrofluorimetric study of porphyrin incorporation into membrane models: evidence for pH effects. *Biochim. Biophys. Acta.* 857:238–250.

Brown, M. S., and J. L. Goldstein. 1976. Receptor-mediated control of cholesterol metabolism. *Science.* 191:150–154.

Candide, C., P. Morliere, J. C. Maziere, S. Goldstein, R. Santus, L. Dubertret, J. P. Reyftmann, and J. Polonovski. 1986. In vitro interaction of the photoactive anticancer porphyrin derivative photofrin II with low density lipoprotein, and its delivery to cultured human fibroblasts. *FEBS Lett.* 207:133–138.

Carr, A. C., M. C. Myzak, R. Stocker, M. R. McCall, and B. Frei. 2000. Myeloperoxidase binds to low-density lipoprotein: potential implications for atherosclerosis. *FEBS Lett.* 487:176–180.

Connors, K. A. 1990. Chemical Kinetics. VCH Publishers, New York.

Cunderlikova, B., M. Kongshaug, L. Gangeskar, and J. Moan. 2000. Increased binding of chlorine(6) to lipoproteins at low pH values. *Int. J. Biochem. Cell. Biol.* 32:759–768.

de Smidt, P. C., A. J. Versluis, and T. J. van Berkel. 1993. Properties of incorporation, redistribution, and integrity of porphyrin-low-density lipoprotein complexes. *Biochemistry.* 32:2916–2922.

de Vries, H. E., A. C. Moor, T. M. Dubbelman, T. J. van Berkel, and J. Kuiper. 1999. Oxidized low-density lipoprotein as a delivery system for photosensitizers: implications for photodynamic therapy of atherosclerosis. *J. Pharmacol. Exp. Ther.* 289:528–534.

Dougherty, T. J., C. J. Gomer, B. W. Henderson, G. Jori, D. Kessel, M. Korbelik, J. Moan, and Q. Peng. 1998. Photodynamic therapy. *J. Natl. Cancer Inst.* 90:889–905.

Gal, D., P. C. MacDonald, J. C. Porter, and E. R. Simpson. 1981. Cholesterol metabolism in cancer cells in monolayer culture. III. Low-density lipoprotein metabolism. *Int. J. Cancer.* 28:315–319.

Galantai, R., I. Bardos-Nagy, K. Modos, J. Kardos, P. Zavodszky, and J. Fidy. 2000. Serum albumin-lipid membrane interaction influencing the uptake of porphyrins. *Arch. Biochem. Biophys.* 373:261–270.

Halfman, C. J., and T. Nishida. 1972. Method for measuring the binding of small molecules to proteins from binding-induced alterations of physical-chemical properties. *Biochemistry.* 11:3493–3498.

Havel, R. J., H. A. Eder, and J. H. Bragdon. 1955. The distribution and chemical composition of ultracentrifugally separated lipoproteins in human serum. *J. Clin. Invest.* 34:1345–1353.

Henderson, B. W., D. A. Bellnier, W. R. Greco, A. Sharma, R. K. Pandey, L. A. Vaughan, K. R. Weishaupt, and T. J. Dougherty. 1997. An in vivo quantitative structure-activity relationship for a congeneric series of pyropheophorbide derivatives as photosensitizers for photodynamic therapy. *Cancer Res.* 57:4000–4007.

Ho, C. H., D. W. Britt, and V. Hlady. 1996. Human low density lipoprotein and human serum albumin adsorption onto model surfaces studied by total internal reflection fluorescence and scanning force microscopy. *J. Mol. Recognit.* 9:444–455.

Jain, R. K. 1987. Transport of molecules in the tumor interstitium: a review. *Cancer Res.* 47:3039–3051.

Jori, G., M. Beltramini, E. Reddi, B. Salvato, A. Pagnan, L. Ziron, L. Tomio, and T. Tsanov. 1984. Evidence for a major role of plasma lipoproteins as hematoporphyrin carriers in vivo. *Cancer Lett.* 24: 291–297.

Kessel, D. 1986. Porphyrin-lipoprotein association as a factor in porphyrin localization. *Cancer Lett.* 33:183–188.

Kuzelova, K., and D. Brault. 1994. Kinetic and equilibrium studies of porphyrin interactions with unilamellar lipidic vesicles. *Biochemistry.* 33:9447–9459.

Lakowicz, J. R. 1983. Principles of Fluorescence Spectroscopy. Plenum Press, New York.

Lavi, A., H. Weitman, R. T. Holmes, K. M. Smith, and B. Ehrenberg. 2002. The depth of porphyrin in a membrane and the membrane's physical properties affect the photosensitizing efficiency. *Biophys. J.* 82: 2101–2110.

Lee, D. M., and P. Alaupovic. 1974. Physiocochemical properties of low-density lipoproteins of normal human plasma. Evidence for the occurrence of lipoprotein B in associated and free forms. *Biochem. J.* 137:155–167.

Luna, M. C., A. Ferrario, N. Rucker, and C. J. Gomer. 1995. Decreased expression and function of alpha-2 macroglobulin receptor/low density lipoprotein receptor-related protein in photodynamic therapy-resistant mouse tumor cells. *Cancer Res.* 55:1820–1823.

Maman, N., and D. Brault. 1998. Kinetics of the interactions of a dicarboxylic porphyrin with unilamellar lipidic vesicles: interplay between bilayer thickness and pH in rate control. *Biochim. Biophys. Acta.* 1414: 31–42.

Maziere, J. C., P. Morliere, and R. Santus. 1991. The role of the low density lipoprotein receptor pathway in the delivery of lipophilic photosensitizers in the photodynamic therapy of tumours. *J. Photochem. Photobiol. B.* 8:351–360.

Miller, J. W., A. W. Walsh, M. Kramer, T. Hasan, N. Michaud, T. J. Flotte, R. Haimovici, and E. S. Gragoudas. 1995. Photodynamic therapy of experimental choroidal neovascularization using lipoprotein-delivered benzoporphyrin. *Arch. Ophthalmol.* 113:810–818.

Moan, J., C. Rimington, and A. Western. 1985. The binding of dihematoporphyrin ether (photofrin II) to human serum albumin. *Clin. Chim. Acta.* 145:227–236.

Pass, H. I. 1993. Photodynamic therapy in oncology: mechanisms and clinical use. *J. Natl. Cancer Inst.* 85:443–456.

Peterson, G. L. 1977. Simplification of the protein assay method of Lowry et al. which is more generally applicable. *Anal. Biochem.* 83:346–356.

Rensen, P. C., R. L. de Vrueh, J. Kuiper, M. K. Bijsterbosch, E. A. Biessen, and T. J. van Berkel. 2001. Recombinant lipoproteins: lipoprotein-like lipid particles for drug targeting. *Adv. Drug Deliv. Rev.* 47:251–276.

Reyftmann, J. P., P. Morliere, S. Goldstein, R. Santus, L. Dubertret, and D. Lagrange. 1984. Interaction of human serum low density lipoproteins with porphyrins: a spectroscopic and photochemical study. *Photochem. Photobiol.* 40:721–729.

Rudling, M. J., V. P. Collins, and C. O. Peterson. 1983. Delivery of aclacinomycin A to human glioma cells in vitro by the low-density lipoprotein pathway. *Cancer Res.* 43:4600–4605.

Schmidt-Erfurth, U., H. Diddens, R. Birngruber, and T. Hasan. 1997. Photodynamic targeting of human retinoblastoma cells using covalent low-density lipoprotein conjugates. *Br. J. Cancer.* 75:54–61.

Schumaker, V. N., M. L. Phillips, and J. E. Chatterton. 1994. Apolipoprotein B and low-density lipoprotein structure: implications for biosynthesis of triglyceride-rich lipoproteins. *Adv. Protein. Chem.* 45:205–248.

Segrest, J. P., M. K. Jones, H. De Loof, and N. Dashti. 2001. Structure of apolipoprotein B-100 in low density lipoproteins. *J. Lipid. Res.* 42: 1346–1367.

Shaw, J. M., K. V. Shaw, S. Yanovich, M. Iwanik, W. S. Futch, A. Rosowsky, and L. B. Schook. 1987. Delivery of lipophilic drugs using lipoproteins. *Ann. N.Y. Acad. Sci.* 507:252–271.

Vever-Bizet, C., and D. Brault. 1993. Kinetics of incorporation of porphyrins into small unilamellar vesicles. *Biochim. Biophys. Acta.* 1153: 170–174.

Vitols, S., C. Peterson, O. Larsson, P. Holm, and B. Aberg. 1992. Elevated uptake of low density lipoproteins by human lung cancer tissue in vivo. *Cancer Res.* 52:6244–6247.

Yang, C. Y., S. H. Chen, S. H. Gianturco, W. A. Bradley, J. T. Sparrow, M. Tanimura, W. H. Li, D. A. Sparrow, H. DeLoof, M. Rosseneu, F. S. Lee, Z. W. Gu, A. M. Gotto, and L. Chan. 1986. Sequence, structure, receptor-binding domains and internal repeats of human apolipoprotein B-100. *Nature.* 323:738–742.